

A Predictive Flexibility Aggregation Method for Low Voltage Distribution System Control

Clément Moureau, Thomas Stegen, Mevludin Glavic, Bertrand Cornélusse

Montefiore Institute, University of Liège, Belgium

{clement.moureau}@uliege.be

Abstract—This paper presents a predictive control strategy to manage low-voltage distribution systems. The proposed approach relies on an aggregate of the flexibility at the residential unit level into a three-dimensional chart that represents the injected active and reactive power, and the flexibility cost. First, this method solves a multiparametric optimization problem offline at the residential unit level to aggregate the flexibility of the assets. Then, a semi-explicit model predictive control problem is solved to account for forecasts. By combining the results of these problems with measurements, the method generates the desired flexibility chart. The proposed approach is compatible with real-time control requirements, as heavy computations are performed offline locally, making it naturally parallelizable. By linking real-time flexibility assessment with energy scheduling, our approach enables efficient, low-cost, and privacy-preserving management of low-voltage distribution systems. We validate this method on a low-voltage network of 5 buses by comparing it with an ideal technique.

Index Terms—Low Voltage Distribution System, Residential Unit Flexibility Aggregation, Multiparametric Optimization, Predictive Control

I. INTRODUCTION

In recent years, the penetration of distributed renewable energy sources (DERs) has increased in distribution networks (DNs). Although these support the energy transition and help to meet carbon emission reduction targets, their variability poses significant challenges for the management of DNs. In particular, residential photovoltaic (PV) installations tend to reverse the power flow at high-irradiance periods, which may cause network overvoltage issues. Meanwhile, consumers are often incentivized to accelerate their electrification of heating and mobility, increasing network loading and thus the risk of undervoltage.

Voltage problems will appear more frequently as the penetration of these low-carbon technologies increases, making it harder for network operators to maintain a high-quality power supply. In such situations, expensive measures such as network expansion may become necessary [1], [2]. As an alternative, harnessing the flexibility available at the residential level (inverter-interfaced DERs, stationary batteries, electric vehicles, and heat pumps) has recently gained popularity. This flexibility allows residential units to provide auxiliary services to the grid, with minimal impact on user comfort.

The authors are with the University of Liege, Electrical Engineering and Computer Science Department, Liege, Belgium. This work was supported in part by the F.R.S.-FNRS under the grant of C. Moureau

Even if real-time control of power setpoints may offer an efficient alternative to grid reinforcement, system operators typically cannot directly dispatch these flexibility resources. Moreover, DSOs generally do not own flexible assets, which prevents them from measuring flexibility directly. They must therefore rely on estimates of the available flexibility. An alternative would require residential units (buildings/homes) to report their availability of real-time flexibility [3], [4]. Following the work in [3], we assume that the residential units are equipped with energy management systems (EMS) that could manage energy consumption and estimate the available flexibility. Under this approach, the flexibility should be quantified and communicated to the DSO in a way that enables seamless integration into existing system operations [3]. To reduce the complexity induced by the coordination of a large number of devices, individual device flexibility charts can be aggregated into a single diagram at each node. This represents the flexibility of a group of assets in a compact and convex form [5].

This paper quantifies flexibility using the concept of a flexible chart, providing the system operator with an overview of the nodal flexibility and the corresponding costs. In particular, this article studies how real-time flexibility assessment and energy scheduling can contribute to both the definition of the cost of flexibility and the effective management of DNs.

We propose the use of multiparametric optimization (MPO), a method to solve constrained optimization problems where some of the parameters vary between bounds [6] as the first step in aggregating the flexibility. This technique provides a mapping of the optimal solution as a function of varying model parameters by dividing the space of parameters into critical regions. These regions are areas in the parameter space with the same active constraints. This step is conducted offline and at the level of a residential unit.

The second step is also solved offline using MPO and is formulated as a semi-explicit model predictive control (MPC). This step accounts for time coupling constraints and forecasts. It involves only one varying parameter.

The third step of the proposed aggregation includes collecting real-time measurements that, combined with the results of the first and second step, generate a three-dimensional flexibility chart (flexibility cost versus active and reactive power) of every residential unit. These functions are presented to a central controller that computes active and reactive power setpoints for each unit. These setpoints are sent back to each unit, where they are implemented through a simple function

evaluation.

A. Related literature review

Many studies have already discussed the idea of leveraging the flexibility of inverter-interfaced generation and loads to improve the management of distribution systems. Most of them have focused on the use of PV inverters only [7]–[9]. Other works extended these concepts to loads, EVs [10], or use several of these simultaneously to provide ancillary services to the grid [11]. This opens the door to new opportunities where prosumers could be compensated for the services they offer to the distribution network through local electricity markets [12] or local energy communities [13]. In [12], a local flexibility market is defined as a platform to trade flexibility in local areas. It proposes an optimization problem to manage disconnectable and shiftable loads as well as generators and batteries.

In [14], a method has been proposed to assess the flexibility of the buildings by evaluating the amount of energy that can be shifted from one time step to another and the cost resulting from this shift. The proposed method is based on the solution of multiple optimal control problems, which is a bottleneck of the method. Other methods make use of implicit MPC strategies to evaluate the flexibility of buildings in the presence of varying electricity prices or uncertainties [4], [15]–[17]. These approaches quantify the flexibility of residential units to offer cost efficient services to the power system while trying to achieve savings in electricity costs for the residential prosumers. In particular, [17] proposed to account for user preferences in addition to the physical constraints before deriving the available flexibility. However, most of these methods are usually not directly applied to solve operational issues in distribution networks. Moreover, they usually do not consider reactive power flexibility.

B. Contributions

The main contributions of this work are:

- The use of MPO for residential units assets flexibility aggregation.
- The use of semi-explicit model predictive control, solved using MPO, to account for time-coupling constraints while integrating forecasts of electricity prices, consumption, and production in flexibility aggregation.
- A scalable and privacy-preserving method for controlling distribution systems.
- An efficient disaggregation method taking advantage of the offline explicit solution to share setpoints among assets.

Overall, the control scheme is compatible with real-time requirements since heavy computations are done offline, while they are fully decentralized (at the level of residential units), making it completely parallelizable.

This paper presents the control architecture in full detail and demonstrates its capabilities using the flexibility of residential unit DERs (PV and BESS), while considerations for load flexibility are left for future work.

This paper is structured as follows. Section II introduces the control strategy. Section IV formulates the offline MPO problem, allowing aggregation of flexibility and cost functions. The semi-explicit MPC problem, which accounts for forecasts and is solved using MPO, is presented in Section III. Section V addresses the real-time evaluation of aggregated charts, central control, and disaggregation. Numerical simulations demonstrating the effectiveness of the proposed method are reported in Section VI. Finally, conclusions are drawn in Section VII.

II. CONTROL STRATEGY OVERVIEW

The goal is to provide the central controller with a mapping of the available flexibility and associated costs as a function of the grid exchanges at each node, allowing optimization of the nodal setpoints. However, rather than solving an offline problem with fixed costs and an unknown future as in [18], forecasts are used to determine the price of flexibility.

Given the online requirements, solving a full horizon problem at each time step is not tractable to determine the price of flexibility. To overcome this issue, the computational burden can be subdivided into operational planning and real-time stages. The former is responsible for optimizing the decisions over a long-term horizon at a market period resolution, while the latter handles setpoints within the current market period.

Inspired by [19] and [20], we propose using a value function as a way to propagate information from operational planning to the real-time optimization stage. In this framework, the operational planning stage uses day-ahead forecasts of PV generation and load to compute the cost-to-go by minimizing the total energy cost over the horizon. The cost-to-go is a value function that summarizes future costs with respect to the system state at the end of the ongoing market period. The real-time controller then solves an optimization problem that incorporates this value-function information and measurements to compute the optimal nodal power exchanges.

As illustrated in Fig. 1, the method consists of three main steps, each operating at a different frequency.

A. Offline Solving of Real-time Policy

In the offline stage, an MPO problem is formulated and solved over a generic 15-minute market period, using a parameterized representation of the cost-to-go as a function of the system state. This yields an explicit mapping between the system parameters and the optimal control policies to be used online.

The key advantage of explicit MPO lies in eliminating repetitive online problem solving, which significantly accelerates online evaluation and enhances robustness [21].

B. Operational Planning (OP)

Every 15 minutes, updated day-ahead forecasts are used to assess the value of the system state at the end of the ongoing 15-minute market interval. This value function is obtained by solving another MPO problem that uses production, consumption, and price predictions, while treating the initial system state as an uncertain parameter.

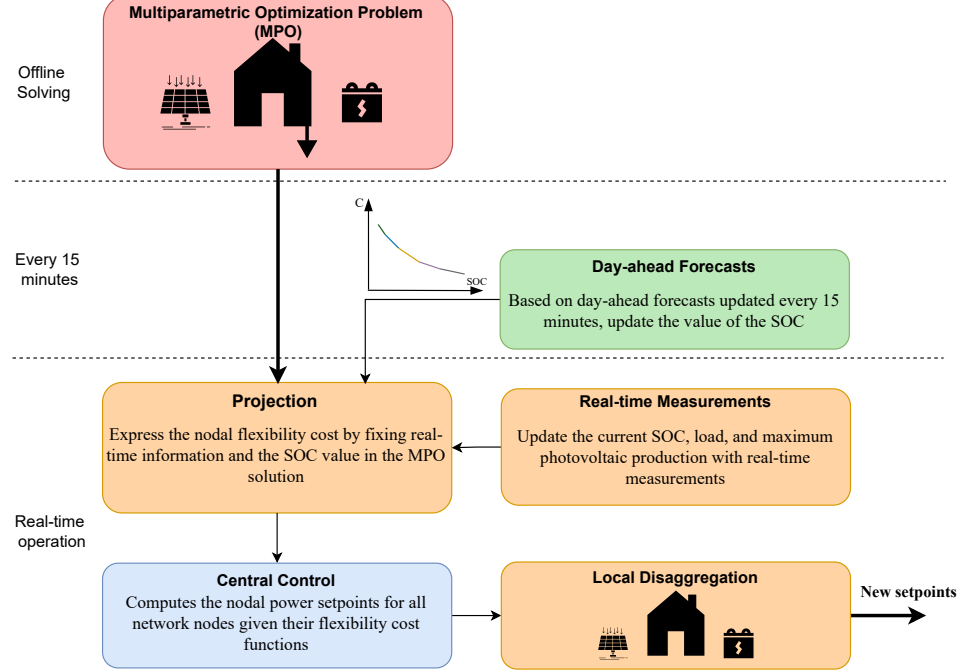


Fig. 1. Simplified representation of the different stages of the proposed control strategy

C. Real-time Control

In real-time, the parameters of the generic MPO are particularized to the current forecast, through the cost-to-go function, and current measurements. Fixing the values of these uncertain parameters in the MPO solution allows to express the instantaneous flexibility and corresponding cost functions in terms of active and reactive power exchanges with the grid. With this information from all network nodes, the central controller computes the optimal setpoints for every node in the network. Finally, the optimal nodal setpoints can be disaggregated among local assets.

Initial efforts in designing the proposed control strategy have been presented in our previous work [18]. To ensure clarity and self-containment, the full model is restated in the following sections. In this paper, we propose a formulation that considers only photovoltaic and batteries, and future work will extend the concept to other devices.

III. OPERATIONNAL PLANNING FORMULATION

Every 15 minutes, an explicit parametric optimization problem is solved using the most recent forecasts. This computation provides a mapping of the SOC value at the end of the 15-minute interval, showing how variations in the initial SOC influence system costs under the forecasted load and production profiles. To capture daily production and consumption patterns, a 23-hour-45-minute horizon divided into N_C intervals is considered. While the first intervals are defined as 15-minute market periods, the interval length is progressively increased for later periods of the day to decrease computational overhead.

A. Objective and Constraints

The objective consists of minimizing the daily energy costs and battery degradation. Constraints define the bounds on the system state and power output of assets.

$$\begin{aligned} \min \sum_{t=1}^{N_C} (\pi_{imp,t} p_{imp,t} + \pi_{exp,t} p_{exp,t}) \Delta \tau_t \\ + \sum_{t=1}^{N_C} \pi_{bat} (p_{ch,t} + p_{dis,t}) \Delta \tau_t \end{aligned} \quad (1)$$

$$\text{s.t. } p_{exp,t} - p_{imp,t} = P_{max,t} + p_{dis,t} - p_{ch,t} - P_{load,t} \quad (2a)$$

$$0 \leq p_{exp,t}, p_{imp,t} \quad (2b)$$

$$0 \leq p_{ch,t} \leq P_{max, bat} \quad (2c)$$

$$0 \leq p_{dis,t} \leq P_{max, bat} \quad (2d)$$

$$SOC_t = SOC_{t-1} + \left(\eta_{ch} p_{ch,t} - \frac{p_{dis,t}}{\eta_{dis}} \right) \frac{\Delta \tau_t}{C_{bat}} \quad (2e)$$

$$SOC_{min} \leq SOC_t \leq SOC_{max} \quad (2f)$$

$$\forall t \in \{1, \dots, N\}$$

$$SOC_0 = \widehat{SOC}_0 \quad (2g)$$

Solving this problem yields a set of regions in \mathbb{R} , \widehat{SOC}_0 being the only varying parameter. Each region is defined by inequalities that specify the values of \widehat{SOC}_0 for which it is active and is characterized by a linear cost function. An example of a resulting piecewise affine function is shown in Fig. 2.

IV. CURRENT MARKET PERIOD MPO FORMULATION

This section introduces the MPO problem associated with the current market period. This period is divided into two

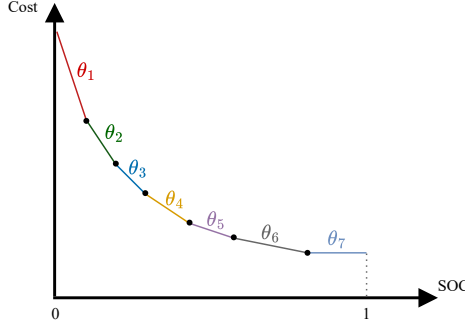


Fig. 2. Example of piecewise affine value function with respect to the SOC at the end of the ongoing market period

sub-intervals, as represented in Fig. 3. The first represents the instantaneous response, lasting 10 seconds, which corresponds to the controller rate. The second reflects the mean expected production and consumption profiles over the remainder of the interval. The duration of this sub-interval, $\Delta\hat{\tau}_r$, decreases after each iteration of the central controller to account for the progression of time without needing to shift the interval at each time step. This brings flexibility to the solution and prevents us from solving a new MPC problem after each time step.

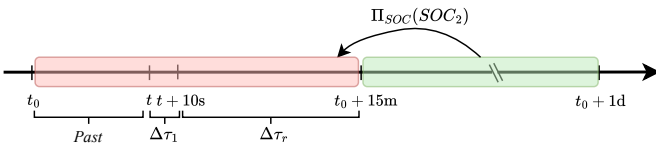


Fig. 3. Timeline of the multiparametric optimization problem, separated into 2 intervals and incorporating a view of the future through Π_{SOC}

A. Objective Function

The objective (3) is to minimize daily energy costs comprising the cost over the current market period (Π_{net}), the impact of real-time action on future costs (Π_{SOC}), reactive power production usage (Π_Q), and battery degradation (Π_{bat}).

$$\min \quad \Pi_{net} + \Pi_Q + \Pi_{bat} + \Pi_{SOC} \quad (3)$$

The energy cost resulting from power exchanges with the grid during this market period is defined as:

$$\Pi_{net} = (p_{imp,1}\Delta\tau_1 + e_{imp,2})\hat{\pi}_{imp} - (p_{exp,1}\Delta\tau_1 + e_{exp,2})\hat{\pi}_{exp} \quad (4)$$

with $p_{imp,1}$ and $p_{exp,1}$ representing the imported and exported powers for the next $\Delta\tau_1$ seconds, and $e_{imp,2}$ and $e_{exp,2}$ being the energy imports and exports for the remainder of the interval.

Then, the cost associated with the SOC value at the end of the ongoing 15-minute market period, Π_{SOC} , is considered. It is modeled as a piecewise linear function of N_s segments.

$$\Pi_{SOC} = \sum_{n=1}^{N_s} \hat{\Theta}_n \Delta S_n \quad (5)$$

Here, $\hat{\Theta}_n$ are the parameters that describe the slopes of each segment. Since the OP is modeled as a linear program, the value function is convex such that:

$$\hat{\Theta}_n \leq \hat{\Theta}_{n+1}, \quad \forall n \in \{1, \dots, N_s - 1\} \quad (6)$$

The breakpoints of the SOC domain are denoted by \hat{S}_n , while the auxiliary variables ΔS_n are introduced to determine the location of the terminal SOC, SOC_2 , within the value function. Eq. (7) establishes the relationship between SOC_2 , the smallest breakpoint \hat{S}_1 , and the cumulative increments ΔS_n , thus ensuring consistency.

$$SOC_2 = \hat{S}_1 + \sum_{n=1}^{N_s} \Delta S_n \quad (7)$$

$$0 \leq \Delta S_n \leq \hat{S}_{n+1} - \hat{S}_n, \quad \forall n \in \{1, \dots, N_s\} \quad (8)$$

$$\hat{S}_n \leq \hat{S}_{n+1} \quad \forall n \in \{1, \dots, N_s\} \quad (9)$$

Finally, two penalty terms are added, the cost associated with instantaneous reactive power usage in the PV (q_{PV}) and the battery (q_{bat}):

$$\Pi_Q = \pi_Q (|q_{bat}| + |q_{PV}|) \Delta\tau_1 \quad (10)$$

and with battery degradation due to charging and discharging:

$$\Pi_{bat} = \pi_{bat} (|p_{bat,1}| \Delta\tau_1 + |e_{bat,2}|) \quad (11)$$

B. Power and Energy Balance Constraints

The power balance constraints define the power exchanges between the grid and the node.

$$p_{exp,1} - p_{imp,1} = p_{PV} + p_{dis,1} - p_{ch,1} - \hat{p}_{load,1} \quad (12)$$

$$p_{exp,1}, p_{imp,1}, p_{ch,1}, p_{dis,1} \geq 0$$

$$q_{exp,1} - q_{imp,1} = q_{PV,1} + q_{bat,1} - \hat{q}_{load,1} \quad (13)$$

$$q_{exp,1}, q_{imp,1} \geq 0$$

Similarly to the power balance, an energy balance can be performed regarding the second part of the 15-minute interval.

$$e_{exp,2} - e_{imp,2} = \hat{e}_{PV,2} + e_{dis,2} - e_{ch,2} - \hat{e}_{load,2} \quad (14)$$

$$e_{exp,2}, e_{imp,2}, e_{ch,2}, e_{dis,2} \geq 0$$

In addition to the previous balances, two parameters, describing the total power exchanges between the node and the grid during the first interval, are also defined, \hat{P}_{grid} and \hat{Q}_{grid} . As explained in [18], introducing these additional parameters allows to express the instantaneous flexibility and corresponding cost functions with respect to active and reactive power exchanges with the grid.

$$\hat{P}_{grid} = p_{exp,1} - p_{imp,1} \quad (15)$$

$$\hat{Q}_{grid} = q_{exp,1} - q_{imp,1} \quad (16)$$

Remark I (Reactive Power). The reactive power balance is only considered for the first time step. It is seen as a way to improve the control of DNs in real time, and its impact on the future is neglected.

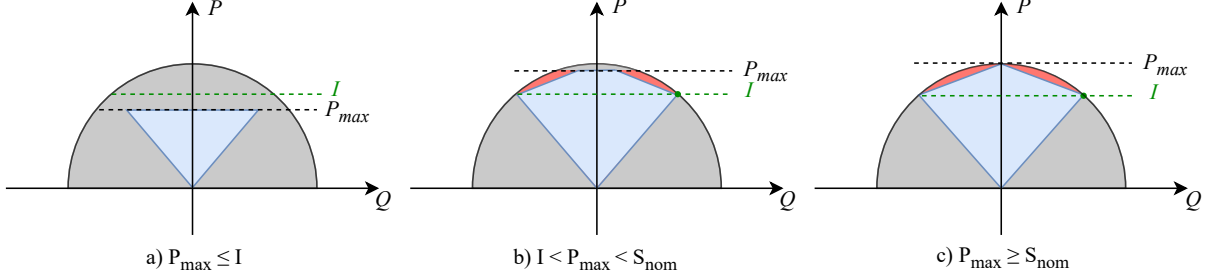


Fig. 4. Approximation of the PV flexibility chart depending on P_{max} [18]

C. Asset Constraints

1) *Power Constraints*: The flexibility limits of assets such as PV and BESS are constrained by inverter apparent power boundaries, which can be approximated using tailored inner polygonal representations to ensure feasibility and efficient MPO solving. These polygonal approximations must capture the time-varying power capabilities of each component, resulting in flexibility charts of different shapes depending on technical limits and operating conditions.

In the case of a PV installation, power limits depend on the inverter's apparent power, the irradiance, and grid codes. The operating point (p_{PV}, q_{PV}) must satisfy the following constraints:

$$p_{PV}^2 + q_{PV}^2 \leq S_{nom,PV}^2, \quad (17)$$

$$0 \leq p_{PV} \leq \hat{P}_{max,PV}, \quad (18)$$

$$-p_{PV}/3 \leq q_{PV} \leq p_{PV}/3. \quad (19)$$

Similarly, for a BESS, the constraints are:

$$p_{bat}^2 + q_{bat}^2 \leq S_{nom,bat}^2 \quad (20)$$

$$SOC_1 = \hat{SOC} + \left(\eta_{ch} p_{ch,1} - \frac{p_{dis,1}}{\eta_{dis}} \right) \frac{\Delta\tau_1}{C_{bat}} \quad (21)$$

$$SOC_2 = SOC_1 + \left(\eta_{ch} e_{ch,2} - \frac{e_{dis,2}}{\eta_{dis}} \right) \frac{1}{C_{bat}} \quad (22)$$

with,

$$SOC_{min} \leq \hat{SOC} \leq SOC_{max} \quad (23)$$

$$SOC_{min} \leq SOC_t \leq SOC_{max} \quad \forall t \in \{1, 2\} \quad (24)$$

In the previous equations, (17) and (20) are quadratic and must be linearized to be integrated in the multiparametric problem. In particular, the PV flexibility charts can be approximated as represented in Fig. 4 depending on the value of the maximum PV output. Similarly, a possible linearization of (20) is presented in Fig. 5.

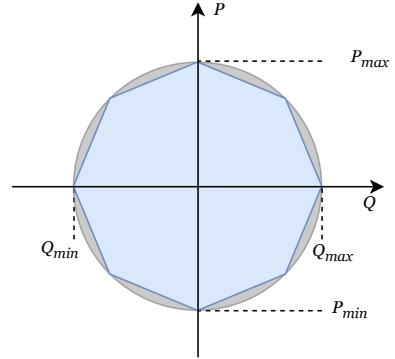


Fig. 5. Example of approximation of the BESS flexibility chart

2) *Energy Constraints*: For the second subinterval, the constraints are expressed in terms of energy rather than power since the duration of the time interval $\Delta\hat{\tau}_r$ is changing. Indeed, working with power would require multiplying variables (e.g., p_{ch} and p_{dis}) by a parameter ($\Delta\hat{\tau}_r$) to compute the SOC, making the constraints nonlinear. For this, we must scale the battery's energy limits based on the remaining time within the interval.

$$0 \leq e_{dis,2} \leq P_{dis,max} \Delta\hat{\tau}_r \quad (25)$$

$$0 \leq e_{ch,2} \leq P_{ch,max} \Delta\hat{\tau}_r \quad (26)$$

$$0 \leq \Delta\hat{\tau}_r \leq \Delta\tau_2 \quad (27)$$

with $\Delta\tau_2$ being the maximum length of the interval, 15 minutes minus 10 seconds.

D. Solving

The previous problem is solved offline, once and for all. This provides a set of polyhedra in $\mathbb{R}^{|\mathcal{P}|}$, where \mathcal{P} is the set of varying parameters.

Each polyhedron is defined by a list of linear inequalities (28) and is characterized by its associated cost function $f_r := \mathbb{R}^{|\mathcal{P}|} \mapsto \mathbb{R}$ (29) and linear optimal policy $\mathbf{G}_r := \mathbb{R}^{|\mathcal{P}|} \mapsto \mathbb{R}^{|\mathcal{P}|}$ (30). These regions, along with their corresponding policies and cost functions, are stored to be used in real-time. The set of all critical regions is denoted \mathcal{R} .

$$\mathbf{A}_r \mathbf{x} \leq \mathbf{b}_r, \quad \forall r \in \mathcal{R} \quad (28)$$

$$\Pi_r = f_r(\mathbf{x}), \quad \forall r \in \mathcal{R} \quad (29)$$

$$\mathbf{u}_r^* = \mathbf{G}_r(\mathbf{x}), \quad \forall r \in \mathcal{R} \quad (30)$$

where \mathbf{x} is a vector collecting the system parameters and \mathbf{u}^* the vector of optimal decision variables.

V. REAL-TIME CONTROL

In real-time, the local controller has to provide the right instantaneous cost functions to the central controller. The solution of the offline MPO provides the optimal system costs Π^* and decision variables \mathbf{u}^* as a function of the uncertain parameters. By measuring the system parameters (SOC, load, and MPP), estimating the PV production and load for the remaining of the 15-minute interval, and imposing the value function computed by the operational planning stage, most of these parameters can be determined. This allows the cost function to be expressed in terms of active and reactive power exchanges with the grid only. After collecting this information from all nodes, the central controller computes the optimal nodal setpoints and communicates them to the local controllers responsible for disaggregation.

A. Online Projection

The offline multiparametric problem divides the parameter space into regions, each characterized by different cost functions and optimal policies. To express these functions with respect to the power exchanges with the grid, all parameters except \hat{P}_{grid} and \hat{Q}_{grid} can be fixed inside the explicit solution. This results in a set of functions in which only \hat{P}_{grid} and \hat{Q}_{grid} are allowed to vary.

By definition, a region is active if it contains the point defined by all uncertain parameters. Although this point remains unknown at this stage, the set of potentially active CRs can be restricted to those that are consistent with the fixed parameters values. To identify which critical regions could be active, it is necessary to locate all regions in \mathcal{R} that intersect the subspace described after fixing the values of the following parameters: \hat{S}_n , $\hat{\Theta}_n$, \hat{p}_{load} , \hat{q}_{load} , SOC , $\hat{p}_{max,PV}$, $\hat{\pi}_{exp}$, $\hat{\pi}_{imp}$ and $\Delta\hat{r}_r$.

Each CR is defined by a constraint set $\mathbf{A}_r \mathbf{x} \leq \mathbf{b}_r$. Fixing some parameters in \mathbf{x} allows to subtract their contributions to \mathbf{b}_r using the associated columns in \mathbf{A}_r .

$$\bar{\mathbf{b}}_r \leftarrow \mathbf{b}_r - \mathbf{A}_{r,i} \mathbf{x}_i \quad \forall i \text{ fixed} \quad (31)$$

$$\bar{\mathbf{A}}_r \leftarrow \mathbf{A}_{r,j} \quad \forall j \neq i \quad (32)$$

$$\bar{\mathbf{x}} \leftarrow \mathbf{x}_j \quad \forall j \neq i \quad (33)$$

This results in a reduced linear system that involves fewer parameters. However, the number of critical regions remains the same. To reduce it, rows of the resulting matrix $\bar{\mathbf{A}}_r$ with zero coefficients are separated from the others. The system feasibility is then verified by checking if the corresponding entries in $\bar{\mathbf{b}}_r$ are positive. If any of them are negative, at least one inequality in $\bar{\mathbf{A}}_r \bar{\mathbf{x}} \leq \bar{\mathbf{b}}_r$ cannot be satisfied for any values of \hat{P}_{grid} and \hat{Q}_{grid} . Otherwise, the new constraint set defines a polyhedron in \mathbb{R}^2 which is a potentially active region.

$$\bar{\mathbf{A}}_r \begin{bmatrix} \hat{P}_{grid} \\ \hat{Q}_{grid} \end{bmatrix} \leq \bar{\mathbf{b}}_r \quad (34)$$

Iterating over all regions in \mathcal{R} , a set of polygonal critical regions is obtained. We denote this new set as $\bar{\mathcal{R}}$. Overall, this

process consists of fixing some parameter values and verifying whether the system remains feasible. This projection step reduces the number of unknown parameters, and consequently the number of potentially active regions.

Figure 6 represents an example of such a set with \hat{P}_{grid} and \hat{Q}_{grid} being the only two remaining parameters. Each region is associated with a linear cost function, such that an aggregate cost function $f_j(\hat{P}_{grid}, \hat{Q}_{grid})$ is defined. These critical regions and corresponding cost functions are communicated to the central controller.

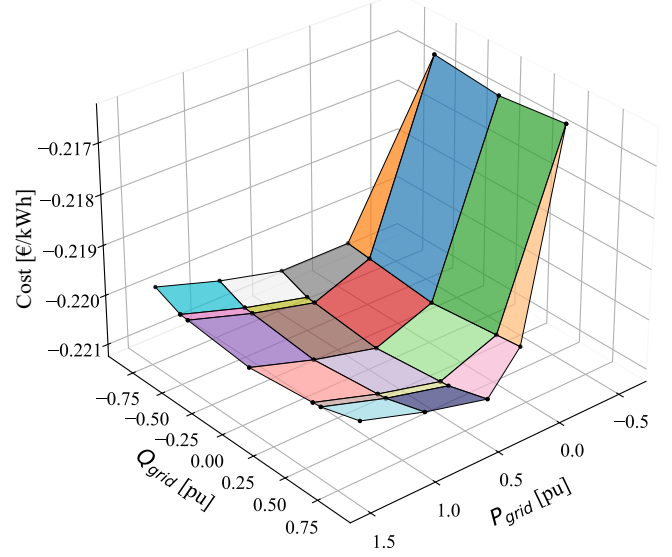


Fig. 6. Cost function in the $P_{grid} - Q_{grid}$ plane for example of parameters

B. Central Optimization

The relaxed *Branch Flow Model* [22] is used to represent a radial LV distribution network.

1) *Objective:* The objective function is formulated as the minimization of the sum of the local and loss costs:

$$\min_{p,q} \sum_j f_j(p_j, q_j) + \pi_l \sum_{(ij) \in \mathcal{E}} R_{ij} l_{ij} \quad (35)$$

where π_l is the cost associated with network losses.

2) *Branch Flow Constraints:* Branch flow constraints describe the coupling between nodal voltages and power exchanges.

$$p_j = \sum_{(jk) \in \mathcal{E}} p_{jk} - \sum_{(ij) \in \mathcal{E}} (p_{ij} - R_{ij} l_{ij}), \quad \forall j \in \mathcal{N}, \quad (36)$$

$$q_j = \sum_{(jk) \in \mathcal{E}} q_{jk} - \sum_{(ij) \in \mathcal{E}} (q_{ij} - X_{ij} l_{ij}), \quad \forall j \in \mathcal{N}, \quad (37)$$

$$v_j = v_i - 2(R_{ij} p_{ij} + X_{ij} q_{ij}) + (R_{ij}^2 + X_{ij}^2) l_{ij}, \quad \forall (i, j) \in \mathcal{E}, \quad (38)$$

$$l_{ij} \geq \frac{p_{ij}^2 + q_{ij}^2}{v_i}, \quad \forall (i, j) \in \mathcal{E} \quad (39)$$

3) *Feasible Set*: The aggregated flexibility of all local assets defines the feasibility set.

$$(p_j, q_j) \in \mathcal{U}_j, \quad \forall j \in \mathcal{N} \quad (40)$$

where \mathcal{U}_j is the union of the polygons in $\bar{\mathcal{R}}$.

4) *Network Constraints*: Voltage levels must stay within a predefined range. This constraint is defined as:

$$0.95^2 \leq v_j \leq 1.05^2, \quad \forall j \in \mathcal{N} \quad (41)$$

C. Disaggregation of Power Setpoints

The disaggregation process is similar to the cost function evaluation. Power setpoints (p_j, q_j) for each residential unit are computed and communicated by the central controller as the optimal power exchange for a specific node. This power must be shared between the assets at minimal cost. This is performed by fixing the remaining varying parameters of \mathbf{x} in (42), \hat{P}_{grid} and \hat{Q}_{grid} . This further enables the identification of the region in which the desired operating point lies.

Mathematically, this comes back to identify the region in \mathcal{R}' for which the following inequalities are satisfied:

$$\bar{\mathbf{A}}_r \begin{bmatrix} \hat{P}_{grid} \\ \hat{Q}_{grid} \end{bmatrix} \leq \bar{\mathbf{b}}_r, \quad \forall r \in \mathcal{R}' \quad (42)$$

The local cost is evaluated using (29) within the corresponding critical region, and the optimal policy from (30) specifies the setpoints of each asset.

VI. SIMULATION RESULTS

In this paper, we compare the proposed strategy with an omniscient one that computes the optimal behavior for each asset, knowing the future of all residential units, similar to operational planning. Comparisons are made on a 5-node single-feeder network. We assume that all houses in the neighborhood have the same irradiance profile, but each one has a different random load profile. The production profile is one of a typical summer day in Belgium. In this paper, only batteries and photovoltaics are considered, but the method could easily be extended to other types of flexible assets. The multiparametric toolbox from *YALMIP* available in MATLAB R2024a [23] is used to solve parametric optimization problems. The central optimization problem is formulated using Pyomo [24] and solved with Ipopt [25].

A. Results

We consider a simplified situation in which only one feeder is considered. This allows for comparing the proposed strategy with an optimal case, optimizing the local costs and network constraints in one large optimization problem, which is not feasible for large networks. The results for both cases are summarized in Table I.

First, it can be noted that the proposed strategy leads to slightly suboptimal results, which was to be expected. Indeed, suppose there is an increase in export prices between two consecutive periods before prices fall lower for the rest of the day. In this case, all nodes would prefer to export during

the second interval. If the network is capable of supporting the maximum output of all nodes, the two methods will be equivalent. However, voltage problems may arise during the second interval, meaning that not all nodes can export as much as they would like. In the omniscient case, the portion of electricity that cannot be exported during the second interval would be exported during the first interval to maximize revenue. In our strategy, this portion would not be exported during the first interval, as the controller cannot predict that there will be voltage problems. Thus, some of the energy will have to be exported at a lower cost, which will reduce revenues.

TABLE I
COST COMPARISON FOR DIFFERENT CONTROL STRATEGIES

	Omniscient	Central
Total Cost (€)	-15.25	-15.09

Table II summarizes the active and reactive production of the assets. It demonstrates the ability of the proposed strategy to limit curtailment, mainly thanks to the use of additional reactive power.

TABLE II
POWER OUTPUT COMPARISON FOR DIFFERENT CONTROL STRATEGIES

	Omniscient	Central
$E_{prod,PV}$ (kWh)	307.09	306.99
$E_{ch,bat}$ (kWh)	155.44	139.29
$E_{dis,bat}$ (kWh)	149.00	134.42
$Q_{prod,tot}$ (kvarh)	3.31	6.29

VII. CONCLUSION

This paper has presented a novel method for managing low-voltage distribution systems based on the aggregated flexibility of residential DERs in a 3-dimensional graph representing injected active power and reactive power, and the associated cost. Based on a set of parameters, aggregated flexibility at the residential unit level is precomputed using offline MPO. An explicit MPC problem was then used to account for the impact of current decisions on future costs. In real-time, only measurements are required to assess the flexibility charts. By shifting most of the computational effort offline, the method significantly reduces the online burden and demonstrates compatibility with real-time requirements. The method was experimentally validated on a 5-bus network with realistic loads and power production profiles. The results demonstrated that the approach converged close to the optimal solution while improving prosumers' privacy.

In future work, the proposed method will be extended to other residential devices such as heat pumps and electric vehicles. Future work will also test this method with other central control algorithms based on online feedback optimization to further improve privacy.

REFERENCES

[1] K. Spiliotis, A. I. R. Gutierrez, and R. Belmans, "Demand flexibility versus physical network expansions in distribution grids," *Applied Energy*, vol. 182, pp. 613–624, 2016.

[2] F. Olivier, P. Aristidou, D. Ernst, and T. Van Cutsem, "Active management of low-voltage networks for mitigating overvoltages due to photovoltaic units," *IEEE Transactions on Smart Grid*, vol. 7, no. 2, pp. 926–936, 2016.

[3] D. Muthirayan, E. Baeyens, P. Chakraborty, K. Poolla, and P. P. Khargonekar, "A minimal incentive-based demand response program with self reported baseline mechanism," *IEEE Transactions on Smart Grid*, vol. 11, no. 3, pp. 2195–2207, 2019.

[4] J. Gasser, H. Cai, S. Karagiannopoulos, P. Heer, and G. Hug, "Predictive energy management of residential buildings while self-reporting flexibility envelope," *Applied Energy*, vol. 288, p. 116653, 2021.

[5] F. L. Müller, J. Szabó, O. Sundström, and J. Lygeros, "Aggregation and disaggregation of energetic flexibility from distributed energy resources," *IEEE Transactions on Smart Grid*, vol. 10, no. 2, pp. 1205–1214, 2019.

[6] I. Pappas, D. Kenefaké, B. Burnak, S. Avraamidou, H. S. Ganesh, J. Katz, N. A. Diangelakis, and E. N. Pistikopoulos, "Multiparametric programming in process systems engineering: Recent developments and path forward," *Frontiers in Chemical Engineering*, vol. 2, p. 620168, 2021.

[7] A. Cagnano and E. De Tuglie, "Centralized voltage control for distribution networks with embedded PV systems," *Renewable Energy*, vol. 76, pp. 173–185, 2015.

[8] B. Ebwank, C. Moureau, M. Glavic, B. Cornélusse, and A. Colot, "A hardware-in-the-loop testbench for voltage control in active distribution networks." Institute of Electrical and Electronics Engineers (IEEE), In press.

[9] X. Su, M. A. S. Masoum, and P. J. Wolfs, "Optimal PV inverter reactive power control and real power curtailment to improve performance of unbalanced four-wire LV distribution networks," *IEEE Transactions on Sustainable Energy*, vol. 5, no. 3, pp. 967–977, 2014.

[10] K. Knezović, M. Marinelli, P. Codani, and Y. Perez, "Distribution grid services and flexibility provision by electric vehicles: A review of options," in *2015 50th International Universities Power Engineering Conference (UPEC)*, 2015, pp. 1–6.

[11] M. Obi, T. Slay, and R. Bass, "Distributed energy resource aggregation using customer-owned equipment: A review of literature and standards," *Energy Reports*, vol. 6, pp. 2358–2369, 2020.

[12] P. Olivella-Rosell, E. Bullich-Massagué, M. Aragüés-Peñaiba, A. Sumper, S. Ø. Ottesen, J.-A. Vidal-Clos, and R. Villafáfila-Robles, "Optimization problem for meeting distribution system operator requests in local flexibility markets with distributed energy resources," *Applied energy*, vol. 210, pp. 881–895, 2018.

[13] H. Nagpal, I.-I. Avramidis, F. Capitanescu, and A. G. Madureira, "Local energy communities in service of sustainability and grid flexibility provision: Hierarchical management of shared energy storage," *IEEE Transactions on Sustainable Energy*, vol. 13, no. 3, pp. 1523–1535, 2022.

[14] R. De Coninck and L. Helsen, "Quantification of flexibility in buildings by cost curves—methodology and application," *Applied Energy*, vol. 162, pp. 653–665, 2016.

[15] E. Vrettos, K. Lai, F. Oldewurtel, and G. Andersson, "Predictive control of buildings for demand response with dynamic day-ahead and real-time prices," in *2013 European Control Conference (ECC)*. IEEE, 2013, pp. 2527–2534.

[16] J. Silvente, G. M. Kopanos, E. N. Pistikopoulos, and A. Espuña, "A rolling horizon optimization framework for the simultaneous energy supply and demand planning in microgrids," *Applied Energy*, vol. 155, pp. 485–501, 2015.

[17] P. Munankarmi, X. Jin, F. Ding, and C. Zhao, "Quantification of load flexibility in residential buildings using home energy management systems," in *2020 American control conference (ACC)*. IEEE, 2020, pp. 1311–1316.

[18] C. Moureau, T. Stegen, and B. Cornélusse, "Residential-level flexibility aggregation for voltage control in active distribution networks," in *2025 IEEE Kiel PowerTech*, 2025, pp. 1–6.

[19] J. Dumas, S. Dakir, C. Liu, and B. Cornélusse, "Coordination of operational planning and real-time optimization in microgrids," *Electric Power Systems Research*, vol. 190, p. 106634, 2021.

[20] R. Kumar, M. J. Wenzel, M. J. Ellis, M. N. ElBSat, K. H. Drees, and V. M. Zavala, "A stochastic dual dynamic programming framework for multiscale mpc," *IFAC-PapersOnLine*, vol. 51, no. 20, pp. 493–498, 2018.

[21] E. N. Pistikopoulos, V. Dua, N. A. Bozinis, A. Bemporad, and M. Morari, "On-line optimization via off-line parametric optimization tools," *Computers & Chemical Engineering*, vol. 26, no. 2, pp. 175–185, 2002.

[22] M. Farivar and S. H. Low, "Branch flow model: Relaxations and convexification—part i," *IEEE Transactions on Power Systems*, vol. 28, no. 3, pp. 2554–2564, 2013.

[23] J. Lofberg, "Yalmip: A toolbox for modeling and optimization in matlab," in *2004 IEEE international conference on robotics and automation (IEEE Cat. No. 04CH37508)*. IEEE, 2004, pp. 284–289.

[24] W. E. Hart, J.-P. Watson, and D. L. Woodruff, "Pyomo: modeling and solving mathematical programs in python," *Mathematical Programming Computation*, vol. 3, no. 3, pp. 219–260, 2011.

[25] A. Wächter and L. T. Biegler, "On the implementation of an interior-point filter line-search algorithm for large-scale nonlinear programming," *Mathematical programming*, vol. 106, no. 1, pp. 25–57, 2006.